Geomechanics and Engineering, *Vol. 21, No. 6 (2020) 513-525*
DOI: https://doi.org/10.12989/gae.2020.21.6.513

Reliability analysis of slopes stabilised with piles using response surface method

Ramanandan Saseendran* and Dodagoudar G. R.[a]

Geotechnical Engineering Division, Department of Civil Engineering, Indian Institute of Technology Madras, Chennai - 600036, India

(Received March 3, 2020, Revised April 16, 2020, Accepted April 28, 2020)

Abstract. Slopes stabilised with piles are seldom analysed considering uncertainties in the parameters of the pile-slope system. Reliability analysis of the pile-slope system quantifies the degree of uncertainties and evaluates the safety of the system. In the present study, the reliability analysis of a slope stabilised with piles is performed using the first-order reliability method (FORM) based on Hasofer-Lind approach. The implicit performance function associated with the factor of safety (FS) of the slope is approximated using the response surface method. The analyses are carried out considering the design matrices formulated based on both the 2^k factorial design augmented with a centre run (2^k fact-centred design) and face-centered cube design (FCD). The finite element method is used as the deterministic model to compute the FS of the pile-slope system. Results are compared with the results of the Monte Carlo simulation. It is observed that the optimum location of the row of piles is at the middle of the slope to achieve the maximum FS. The results show that the reliability of the system is not uniform for different pile configurations, even if the system deterministically satisfies the target factor of safety (FS_t) criterion. The FS_t should be selected judiciously as it is observed that the reliability of the system changes drastically with the FS_t level. The results of the 2^k fact-centred design and FCD are in good agreement with each other. The procedure of the FCD is computationally costly and hence the use of 2^k fact-centred design is recommended, provided the response of the system is sufficiently linear over the factorial space.

Keywords: slope stability; piles; uncertainty; reliability; Hasofer-Lind; finite element method; Monte Carlo simulation; response surface method; FCD; 2^k factorial design

1. Introduction

Piles have been used extensively to stabilise potentially unstable soil slopes or to increase the stability of slopes. Some successful cases of slope stabilisation using piles have been reported by Ito and Matsui (1975), Poulos (1995), Smethurst and Powrie (2007), Yu *et al*. (2014) and Zhou *et al*. (2014). One of the performance criteria in the design of pile-slope system is that the factor of safety (*FS*) of the system should be more than a specified target factor of safety (FS_t). The limit equilibrium (LE) methods have been widely used for the computation of the *FS* of the pile-slope system by modifying the LE equations to incorporate the resistance offered by the piles. The approach of Ito and Matsui (1975) has been used extensively to compute the resistance provided by the piles (Ito and Matsui 1981, Hassiotis *et al.* 1997, Shin *et al*. 2006, Li *et al.* 2015). An extension of the Ito and Matsui (1975) approach was proposed by He *et al.* (2015) considering the soil arching between two neighbouring piles. The LE methods have also been used by Lee *et al.* (1995) and Poulos (1995), wherein the pile response was analysed based on boundary element method. Another approach that has been in use to analyse the stability of pile-slope systems is the limit analysis method (Ausilio *et al*. 2001, Nian *et al*. 2008, Li *et al*. 2012, Xu *et al*. 2018). The location of the slip circle has to be assumed usually in all these approaches. Moreover, the stability analysis of the slope and analysis of the pile response are uncoupled in the LE and limit analysis methods. Both the pile response and stability of the slope are analysed simultaneously using the numerical methods like the finite element method (FEM) or finite difference method (FDM). The continuum-based numerical approaches are also attractive as they can explicitly take into account the material nonlinearity, the variation in stiffness of both the pile and the soil and the soil stratigraphy (Ni *et al*. 2018c). The *FS* of the pile-slope system is computed using the strength reduction method (SRM) when numerical analyses are used. The FEM (Cai and Ugai 2000, Ho 2015, 2017) and FDM (Won *et al*. 2005, Wei and Cheng 2009, Ellis *et al*. 2010, Li *et al*. 2011) based analyses are increasingly being used to evaluate the stability of pile-slope systems.

The methods of analysis mentioned above are all deterministic and do not consider the uncertainties associated with the soil and pile parameters involved in the stability of pile-slope systems. The reliability or probability of failure (P_f) of systems varies with the variation in the degree of uncertainties involved in the analysis (Zhang *et al*. 2017). It is noted from Ruiz (1984) that the reliability of piles subjected to random static lateral loads designed in accordance with the accepted regulations vary across

*Corresponding author, Research Scholar
E-mail: ramanandans@gmail.com
[a]Professor

http://www.techno-press.org/?journal=gae&subpage=7
ISSN: 2005-307X (Print), 2092-6219 (Online)

different sites and is also not uniform. Notwithstanding the degree of the uncertainties and the effects thereof on the performance of the system, the reliability of slopes stabilised with piles has not been rigorously studied, except by Li and Liang (2014) and Zhang *et al*. (2017). Li and Liang (2014) modified the LE method to incorporate a load transfer factor as a measure of the arching between the piles. The load transfer factor as proposed by Joorabchi (2011) is used. This formed the deterministic model for the study which was coded into a computer program UASLOPE. Monte Carlo simulation (MCS) technique is used to compute the P_f. Zhang *et al*. (2017) used the modified form of the simplified Bishop method to incorporate the restoring moment offered by the piles to assess the *FS* of the pile-slope system. The resistance offered by the pile is computed based on the Ito and Matsui (1975) approach. The reliability analyses are carried out by approximating the implicit performance function for the *FS* of the system using the response surface method (RSM). The P_f is computed using the MCS technique. Both these studies use the LE methods as deterministic models combined with the MCS as the basis for the reliability analysis. Though the MCS technique has been used extensively in geotechnical and structural engineering (GuhaRay and Baidya 2014, Mangalathu *et al*. 2018, Ni *et al*. 2018a, Yang and Liu 2018, Ni *et al*. 2020), its use is computationally costlier, especially when the coupled analysis of the three-dimensional (3D) systems are performed using the FEM or FDM. The first-order reliability method (FORM) based on the Hasofer-Lind (H-L) approach (Hasofer and Lind 1974) is an effective alternative to the MCS technique. The H-L method is widely used in the reliability analysis of geotechnical and structural problems (Babu and Singh 2010, Sayed *et al*. 2010, Mandali *et al*. 2011, Yang and Li 2017). However, its application to the reliability analysis of pile-slope systems has not been explored effectively in the literature.

In the present study, the FEM is used as the deterministic model considering the coupled behaviour of the pile-slope system into the reliability analyses. This avoids the need for assuming the potential slip surfaces in advance and searching for the critical slip surface. The prospect of using FORM based on the H-L approach is investigated in this study. The performance function for the *FS* of the system is approximated using the RSM which is an efficient approach to approximate the implicit performance functions and has been used in the reliability analysis of geotechnical systems (Chan and Low 2012, Li *et al*. 2016, Hamrouni *et al*. 2018, Zhu and Yang 2018, Zhang *et al*. 2020). The face-centered cube design (FCD) as well as the 2^k factorial design augmented with a centre run are used to generate the data required for approximating the performance function. The order of the polynomial model used to approximate the performance function is decided based on suitable hypothesis tests on regression coefficients as well as the assessment of the model summary statistics. The results of the H-L method are compared with the results of the MCS technique implemented using the developed performance function.

2. Numerical analysis of the pile-slope system

The 3D finite element (FE) analysis of the pile-slope system is performed using the FE program, ABAQUS. The Mohr-Coulomb plasticity model is used in the analysis for modelling the stress-strain behaviour of the soil, wherein the elastic part of the response is modelled using linear elasticity and the plastic part of the response is modelled using the Mohr-Coulomb failure criterion. The pile is modelled using the linear elastic model. The 8-node linear brick, reduced integration elements with hourglass control (C3D8R) are used for meshing the soil as well as the pile. The C3D8R is a very popular element used for the modelling of pile-soil systems (Ho 2015, Ho 2017, Ni *et al*. 2017). Fixed boundary conditions are applied at the base of the model. The coordinate system used in the present study is shown in Fig. 1. Vertical rollers are used as the boundary condition for the sides of the model, formed by the x-planes. The displacements in the y-direction are restrained on the boundaries corresponding to the y-planes. The analyses are carried out considering only free-head piles. The *FS* of the system is computed using SRM.

The SRM works by gradually reducing the shear strength parameters, cohesion (c) and angle of internal friction (ϕ) of the soil by the strength reduction factor (SRF) until the pile-slope system fails. At the i^{th} value of the SRF (F_i), the values of cohesion (c_i) and angle of internal friction (ϕ_i) of the soil used in the analysis are expressed as

$$c_i = \frac{c}{F_i}$$
$$tan\,\phi = \frac{tan\,\phi}{F_i} \tag{1}$$

The *FS* of the pile-slope system is the value of the SRF at failure. Failure of the slope is defined by the non-convergence of the FE solution and the occurrence of significant increase in the nodal displacements within the FE mesh (Zienkiewicz *et al*. 1975, Ni *et al*. 2016, Tu *et al*. 2016, Ni *et al*. 2018b).

2.1 Validation of the numerical model

The accuracy of the FE model in predicting the *FS* of slopes using SRM is verified by analysing two slopes studied by Griffiths and Lane (1999), viz. a homogenous slope (Slope 1) and a non-homogenous clayey slope with a weak thin layer (Slope 2). These two slope problems are analysed using ABAQUS in the present study. The results thus obtained are compared with those reported by Griffiths and Lane (1999). Further, the results of FE modelling of the soil-pile interaction are validated using the field results of the slope stabilised with piles reported by Carrubba *et al*. (1989).

Griffiths and Lane (1999) analysed the stability of the homogenous slope with an inclination of 26.57°. The geometry of the slope is shown in Fig. 1. The soil properties of the slope are selected to satisfy $c'/\gamma H = 0.05$, where c' is the effective cohesion and γ is the unit weight of the soil. Ho (2014) performed the two-dimensional (2D) and 3D FE

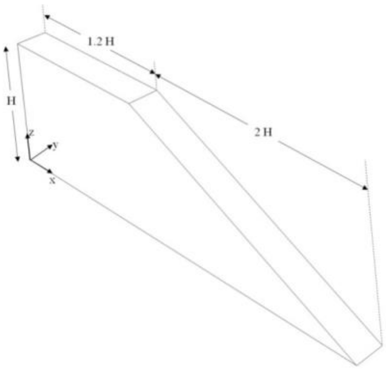

Fig. 1 Geometry of Slope 1 (Griffiths and Lane 1999)

Table 1 Soil properties of Slope 1

Unit weight, γ_s (kN/m^3)	Young's modulus, E_s (MN/m^2)	Poisson's ratio, v_s	Cohesion, c' (kN/m^2)	Friction angle, ϕ' (°)
20	100	0.3	40	20

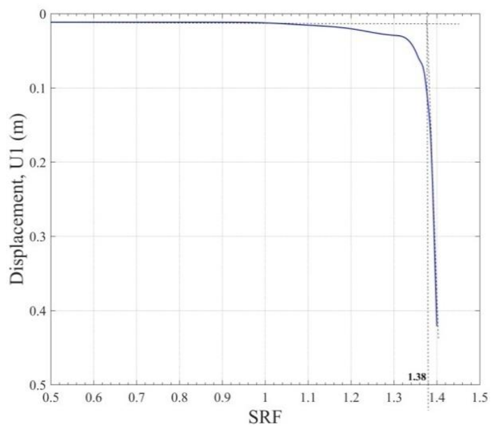

Fig. 2 Displacement versus SRF for Slope 1

Table 2 Comparison of *FS* of Slope 1

Method	ABAQUS 3D	Griffiths and Lane (1999)	Bishop	Morgenstern-Price
FS	1.380	1.400	1.378	1.376

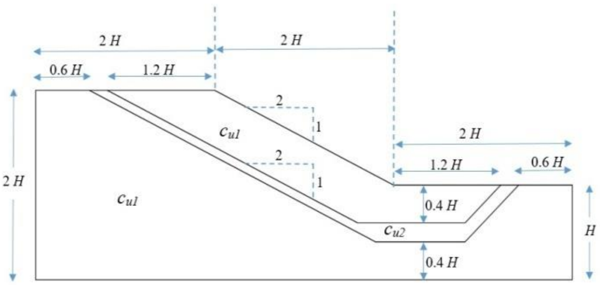

Fig. 3 Geometry of Slope 2 (Griffiths and Lane 1999)

Table 3 Soil properties of Slope 2

Unit weight, γ_s (kN/m^3)	Young's modulus, E_s (MN/m^2)	Poisson's ratio, v_s	Cohesion, c_{ul} (kN/m^2)	Friction angle, ϕ (°)
20	100	0.4	100	0.001

analyses of this slope considering 40 m height of the slope

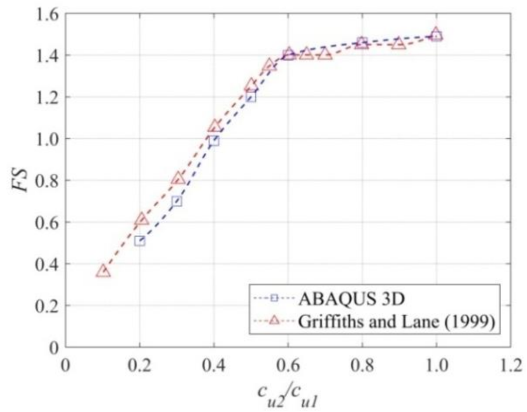

Fig. 4 *FS* versus c_{u2} / c_{u1} for Slope 2

(*H*). The corresponding soil properties are given in Table 1. The 3D FE analysis of the slope is carried out using ABAQUS in this study considering the width of the slope (dimension in the *y* direction) as 10 m. The plot of displacement versus the SRF is shown in Fig. 2. The *FS* of the slope is also computed by Bishop and Morgenstern-Price methods using SLOPE/W program. The results corresponding to the above are given in Table 2. It is observed that the *FS* obtained in the study is slightly lower than the *FS* reported by Griffiths and Lane (1999). However the results are in good agreement with those of the LE methods.

Another example of the non-homogenous slope consisting of clayey soil with a weak thin layer was also presented by Griffiths and Lane (1999). The geometry of the slope is depicted in Fig. 3. The values of *FS* were reported for a range of values of the undrained shear strength of the weak layer (c_{u2}) while maintaining the strength of the remaining soil as $c_{u1} / \gamma H$ = 0.25. In the present study, this slope is analysed using ABAQUS considering a height (*H*) of 20 m for the slope and a width of 10 m. The soil properties as suggested by Griffiths and Lane (1999) are used in the present study and are given in Table 3. A small value of 0.001° for friction angle has been adopted to avoid numerical instability of the mesh.

The slope is analysed for different strength ratios (c_{u2} / c_{u1}) viz. 0.2, 0.3, 0.4, 0.5, 0.6, 0.8 and 1.0. The results of the analysis are shown in Fig. 4. The results are found to be in good agreement with those of Griffiths and Lane (1999).

The validity of the FE model in simulating the soil-pile interaction is assessed by analysing a case study reported by Carrubba *et al*. (1989). Chen and Poulos (1997) and Guo and Ghee (2004) have reproduced the results of the well instrumented full scale field test of Carrubba *et al*. (1989) on a reinforced concrete pile used to stabilise the sliding slope. The test pile had a length of 22 m and was 1.2 m in diameter. The sliding surface was at a depth of 9.5 m from the ground surface with a transition layer of 2 m width. The undrained shear strength of the soil was estimated to be 30 kPa for both the sliding soil and the stable soil. The values of the other parameters for the soil and the pile are as follows:

• The Young's modulus of the soil, E_s is taken as 15 MPa, uniform over the depth.

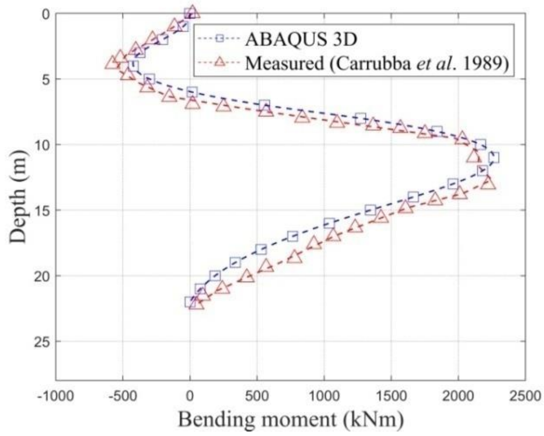

(a) Bending moment along the pile

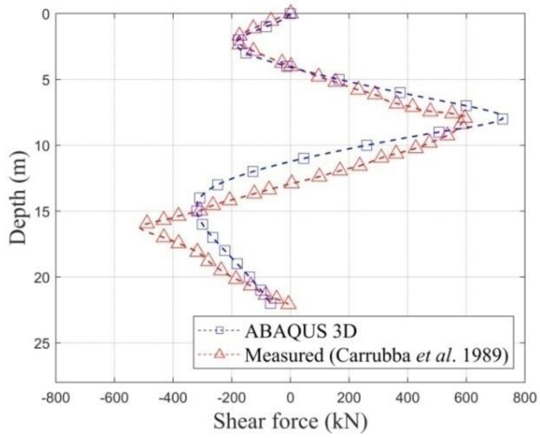

(b) Shear force along the pile

Fig. 5 Results of ABAQUS and measured pile response

Table 4 Soil properties of the pile stabilised slope-system

Unit weight, γ_s (kN/m^3)	Young's modulus, E_s (MN/m^2)	Poisson's ratio, ν_s	Cohesion, c (kN/m^2)	Friction angle, ϕ (°)
18	100	0.33	30	15

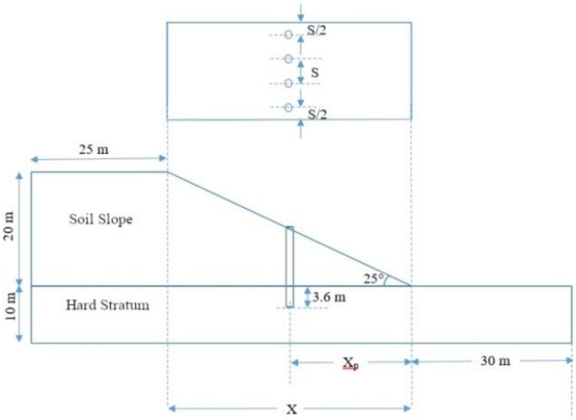

Fig. 6 Geometry of the pile stabilised slope

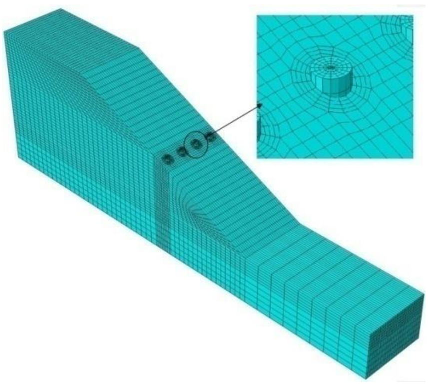
Fig. 7 FE mesh of the pile stabilised slope

• The Young's modulus of the pile, E_c is taken as 20,000 MPa.

• The soil movement profile is considered uniform from the ground surface to the surface of the transition layer with a displacement of 95 mm.

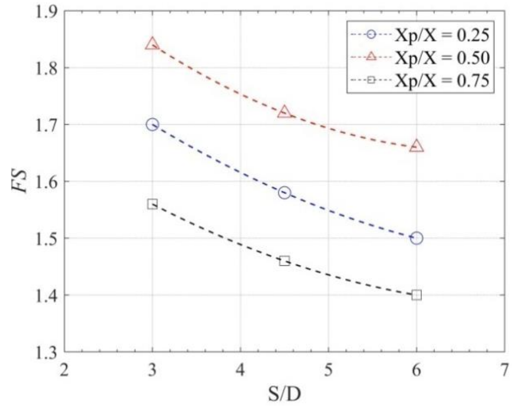

Fig. 8 Variation of FS with S/D ratio

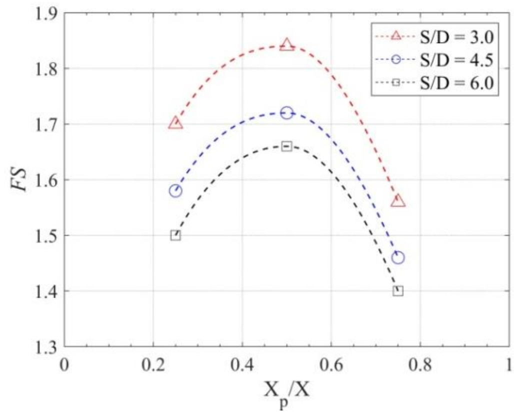

Fig. 9 Effect of location of row of piles on FS

In the present study, the above pile-slope system is modelled using ABAQUS for the purpose of validation of the FE model. A lateral extent of 10 pile diameters, measured from the centre of the pile is sufficient for limiting the influence of the boundary (McGann *et al*. 2012). Hence a domain of 25 m × 25 m is used and discretised for the FE analysis. The ABAQUS results are presented in Fig. 5, together with the measured values (Carrubba *et al*. 1989). The bending moment and shear force profiles are in good agreement with the measured values.

2.2 Stability analysis of a pile stabilised slope

In the present study, the FE based stability analysis of a pile stabilised homogenous soil slope-system is carried out.

Non-homogenous slopes are not considered in the present study to avoid modelling complications and to reduce the computational effort required for the subsequent computationally costly reliability analyses. The slope is underlain by a hard stratum to ensure that only the slope failure should take place. The geometry of the slope is shown in Fig. 6. The height of the soil slope is 20 m and the inclination of the slope is 25° to the horizontal. The material properties of the slope are given in Table 4. The Young's modulus and Poisson's ratio of the hard stratum are taken as 50 GPa and 0.2 respectively. A row of reinforced concrete piles with a pile diameter (D) of 1.2 m is used in the analysis. The Young's modulus of the piles (E_c) is 31 GPa and the Poisson's ratio (ν_c) is 0.2. The analyses are carried out for different locations of the row of piles, denoted by the dimensionless ratio X_p/X, where X_p is the horizontal distance between the row of piles and the toe of the slope and X is the horizontal distance between the crest and toe of the slope. The X_p/X values of 0.25, 0.50, and 0.75 are considered in the study. The piles are embedded into the hard stratum for a length of 3.6 m (i.e., 3D) for all the locations of the row of piles. The length of the piles, consequently, depends on the location of the piles along the slope. The stability analyses are performed for different spacing of the piles in the row, denoted by S/D, where S is the centre-to-centre distance between the piles in the row. The S/D ratio of 3.0, 4.5 and 6.0 are considered in the analysis. The soil is modelled using Mohr-Coulomb plasticity model whereas the pile and hard stratum are modelled using linear elastic behaviour. The FE mesh of the pile-slope system is discretised using C3D8R elements as depicted in Fig. 7.

The influence of spacing of piles in the row on the *FS* of the slope is shown in Fig. 8. It is evident that the *FS* of the pile-slope system increases with decrease in the pile spacing for all the pile locations. It is also found that the rate of increase in the *FS* increases with the decrease in the pile spacing. These observations are consistent with the findings of Cai and Ugai (2000), Won *et al*. (2005), Ho (2015) and Ho (2017). This can be attributed to the fact that the number of piles in the row increases with decrease in the spacing of piles, leading to higher resistance being offered per unit width of the slope to the sliding mass.

The variation of *FS* with location of the row of piles from the toe of the slope is shown in Fig. 9. It is observed that the row of piles should be located at the middle portion of the slope (X_p/X = 0.5) to obtain the maximum *FS* for the pile-slope system. This is also consistent with the results of Cai and Ugai (2000), Won *et al*. (2005), Ho (2015) and Ho (2017). The unsupported slope length is minimum when the piles are placed at the middle of the slope compared to the cases where the piles are placed either near the toe or crest of the slope.

3. Sensitivity analysis

It is important to conduct a screening experiment to understand the sensitivity of the *FS* of the pile-slope system to the uncertainties of the different parameters or factors involved in the stability of the pile-slope system. Such an experiment, also known as sensitivity analysis, helps in identifying the factors, the uncertainties of which may render the deterministic analysis of *FS* erratic. These factors need to be considered as random parameters and should be included in the reliability analysis of the pile-slope system. This also helps in reducing the number of factors to be considered as random variables in the reliability analysis and thereby reducing the number of ABAQUS runs, resulting in a more efficient reliability analysis. Owing to the simplicity, the 'One at a Time' method (Hamby 1994) is adopted in the present study. In the 'One at a Time' method, each of the factors have three factorial levels, the low level denoted by '-1', the centre point denoted by '0' and the high level denoted by '+1'. The factors are varied successively, one at a time, between the respective factorial levels, keeping the other factors at their centre points and the response of the system is evaluated. In the study, the mean value (μ) of the factors is considered as the centre point. The high level and the low level of the factors are considered as μ + 1.65 σ and μ - 1.65 σ respectively, where σ is the standard deviation of the respective parameter. These levels are based on the assumption that all the factors follow normal probability distribution. Hence, the high level has only 5% probability of being exceeded and the low level has 95% probability of being exceeded. This range, therefore takes into account 90% of the uncertainties associated with the factors.

The sensitivity analysis for *FS* of the pile-slope system is carried out for the particular case of X_p/X = 0.5 and S/D

Table 5 COV of the variables considered in the study

Factor	COV (%)	Factor	COV (%)
Unit weight of soil (γ_s)*	9	Unit weight of pile (γ_c)#	5
Young's modulus of soil (E_s)*	15	Young's modulus of pile (E_c)§	5
Poisson's ratio of soil (ν_s)†	15	Poisson's ratio of pile (ν_c)†	5
Cohesion of Soil (c)*	20		
Friction angle of soil (ϕ)*	10		

*Phoon and Kulhawy (1999), #Mandali *et al*. (2011) §Lee *et al*. (2017); †subjectively chosen

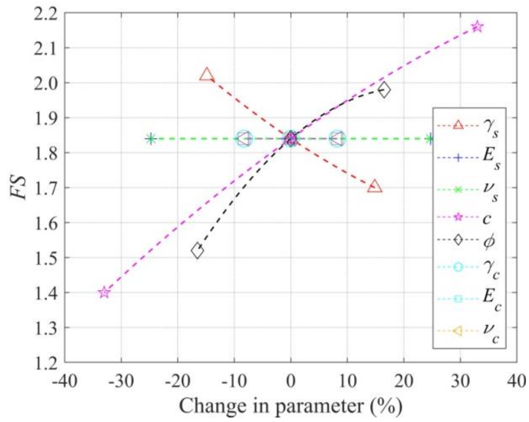

Fig. 10 Spider plot of the sensitivity analysis

= 3. The stability of the pile-slope system is analysed using ABAQUS for each of the combinations of the 'One at a Time' design matrix. Table 5 gives the list of different factors considered in the study, along with their respective coefficient of variation (COV). The geometric parameters related to the piles such as the diameter and length, pile spacing and location of the piles along the slope are considered as deterministic. A better in-situ quality control during construction ensures the uncertainties in these geometric parameters negligible and hence these parameters are treated as deterministic.

A simple and efficient graphic form to present and interpret the results of a sensitivity analysis is the spider plot (Eschenbach 1992, Loucks and Beek 2017). The spider plot facilitates the illustration of the effect of uncertainty of each factor on the *FS* on the same graph. This necessitates the use of a common metric as abscissa to represent the various factorial levels. The use of percent change from the mean values is a convenient metric and hence the same is used in the study. The results of the sensitivity analysis are presented as a spider plot in Fig. 10. It is observed from the spider plot that the *FS* of the pile-slope system is not sensitive to the uncertainties of the Young's modulus and Poisson's ratio of both the soil and pile as well as the unit weight of the pile. Therefore, only the unit weight, cohesion and angle of internal friction of the soil are considered as random variables in the reliability analyses.

4. Reliability analysis

Reliability of an engineered system is defined as the probability that the system satisfies the specified performance criterion. Probability of the complementary event in which the system does not meet the specified criterion is termed as the probability of failure. Failure can be mathematically expressed as

$$g = R - Q < 0 \tag{2}$$

where *R* is the resistance or capacity offered by the system to meet the performance criterion and *Q* is the demand or load on the system. The performance function *g* is a function of several load and resistance variables and is expressed as

$$g(X_1, X_2, ..., X_k) = g(X) \tag{3}$$

where *X* is the *k*-dimensional vector of random variables X_1, X_2, ..., X_k, which involve the different load and resistance variables. The function $g = 0$ defines the limit state, which is the boundary between the safe domain ($g > 0$) and the failure domain ($g < 0$). The P_f is expressed in terms of the performance function as

$$P_f = P[g(X) < 0] \tag{4}$$

If the variables *R* and *Q* are correlated, the P_f can be determined by the computation of the following integral:

$$P_f = \iint\limits_{g(X)<0} f_{RQ}(r,q)\,dq\,dr \tag{5}$$

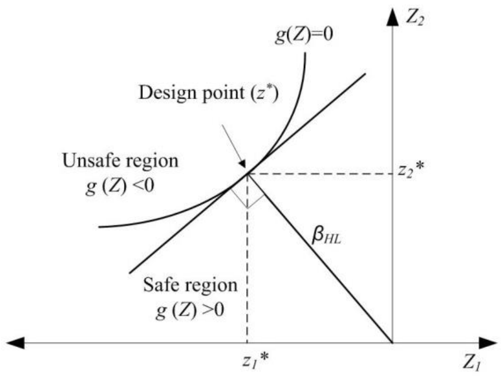

Fig. 11 Performance space in reduced coordinates

where f_{RQ} is the joint probability density function of *R* and *Q*. If *R* and *Q* are statistically independent, marginal probability density functions of *R* and *Q* are used in Eq. (5) instead of f_{RQ}. It is often very difficult to evaluate the multiple integral in Eq. (5) and hence analytical solutions are used to compute the P_f. A commonly used analytical method is the H-L method. The P_f can also be evaluated using simulation techniques like the MCS.

4.1 Hasofer-Lind (H-L) method

The H-L method is applicable only to uncorrelated normal random variables. The method involves the transformation of all the random variables (X_i) in *X* into a reduced form (Z_i) defined as

$$Z_i = \frac{X_i - \mu_{X_i}}{\sigma_{X_i}} (i = 1, 2, ..., k) \tag{6}$$

where μ_{X_i} and σ_{X_i} are the mean and standard deviation of the random variable X_i. The reduced variables have zero mean and unit standard deviation. The Z_i coordinate system is called as the reduced coordinate system. The H-L reliability index (β_{HL}) is defined as the minimum distance from the origin of the reduced coordinate system to the limit state function defined by $g(Z) = 0$ as depicted in Fig. 11. Here *Z* is the *k*-dimensional vector of the reduced form of the random variables. The point which is at the minimum distance from the origin of the reduced coordinate system is called the design point (Z^*). The distance from the origin of the reduced variable space to any point on the limit state function is

$$D = \sqrt{Z_1^2 + Z_2^2 + ... + Z_k^2} = \sqrt{Z^T Z} \tag{7}$$

Determination of the minimum value of *D* which is the value of β_{HL} can now be treated as a constrained minimisation problem with the constraint being $g(Z) = 0$, where $g(Z)$ is the performance function in the reduced coordinate system. The solution of this optimisation problem is sought by using the Lagrangian multiplier method. The Lagrangian is defined as

$$L = D + \lambda g(Z) = \sqrt{Z^T Z} + \lambda g(Z) \tag{8}$$

where λ is the Lagrangian multiplier. At the design point, λ is zero and hence the minimum of L and D is the same. At the minima of L, the partial derivatives of L with respect to the random variables must be zero. This leads to the following:

$$Z = -\frac{DG}{\sqrt{G^T G}}, \quad D = \frac{G^T Z}{\sqrt{G^T G}} \tag{9}$$

where G is the gradient of $g(Z)$. The minimum value of D with the constraint that $g(Z) = 0$ corresponds to β_{HL} which is expressed in the form:

$$\beta_{HL} = \frac{G^{*T} Z^*}{\sqrt{G^{*T} G^*}} \tag{10}$$

where G^* is the value of G computed at the design point. At the outset of the evaluation of β_{HL}, location of the design point is not known and the process proceeds in an iterative manner. The G is normalised into a unit vector α as follows:

$$\alpha = \frac{G}{\sqrt{G^T G}} \tag{11}$$

Then the coordinates of the design point are expressed as

$$Z^* = -\alpha_i^* \beta_{HL} \tag{12}$$

Nowak and Collins (2013) described an algorithm for the evaluation of β_{HL}, called the matrix procedure. It involves the following steps:

- Formulating the limit state function as a function of X.
- Obtaining an initial design point $\{x_i^*\}$ by assuming values for k - 1 of the random variables and then solving $g(X) = 0$ for the remaining random variable.
- Determining the reduced variables Z^* for the design point $\{x_i^*\}$.
- Determining the values of G.
- Calculating estimates of β_{HL} and α.
- The new design point in the reduced variable space is then computed for k - 1 of the variables using $Z_i^* = -\alpha_i\beta_{HL}$.
- The corresponding k - 1 values of the design point are calculated in original coordinates. The value of the remaining random variable is then computed by solving $g(X) = 0$.
- Steps 3 to 6 are repeated until β_{HL} and $\{x_i^*\}$ converge.

It can be observed from the above that the computation of β_{HL} needs an explicitly stated limit state function. But in the case of numerical analyses like FE analyses, such explicit limit state functions are not available. This necessitates the approximation of the limit state function. The RSM is one such approach of learning from data to approximate the limit state function.

4.2 Response surface method

Quite often than not, it becomes necessary to approximate the limit state function because it is difficult to derive a closed form solution for the same. In such cases, a convenient approach is to learn from data comprising of observations of the response of the system 'g' to a set of combinations of possible realisations of the factors affecting the said response. In general, the objective then is to arrive at a mapping from the input vector X to the response g, when N pairs of data $\{x_i, g_i\}$ are available, where i = 1, 2, . . ., N and x denotes a particular realisation of X. The set of N realisations of X can be denoted in the matrix form as $\mathbf{X}$ which is therefore a $N \times k$ matrix and the observations on 'g' constitute a N dimensional vector $\mathbf{g}$. An approximation of the relationship between g and X can then be expressed as

$$g = f(X) + \varepsilon \tag{13}$$

where ε is the statistical error that represents sources of uncertainty not included in f. Multiple linear regression using a suitable method can be used to develop a satisfactory model for Eq. (13). Polynomial regression has been extensively used in the past for reliability analysis of slopes using the RSM (Ji and Low 2012, Zhang *et al*. 2013, Zhang *et al*. 2017). In particular, the widely used second-order polynomial model (Myers *et al*. 2009) is given below:

$$g = \beta_0 + \sum_{j=1}^{k} \beta_j X_j + \sum_{j=1}^{k} \beta_{jj} X_j^2 + \varepsilon \tag{14}$$

The β's are called the partial regression coefficients and are the unknown parameters of the regression model.

4.2.1 Design of experiments

The use of a second-order polynomial model for the approximation of the limit state function requires the experimental design to have the following properties (Myers *et al*. 2009):

- At least three levels of values are taken for each of the factors considered.
- The number of unique design points is at least 1 + 2k + $k(k$ - 1)/ 2.

A very important factorial design is where each of the k factors have two levels: the high level, denoted by '+1' and the low level denoted by '-1'. Such a design, called the 2^k factorial design is often used to fit first-order polynomial models and necessitates 2^k simulation runs. The combinations of the factorial levels for the simulation runs lie at the corner points of a k-dimensional hypercube centred on the combination of the centre points of all the factors. The design matrix of the 2^k factorial design with three factors X_1, X_2 and X_3 correspond to the runs 1-8 as given in Table 6.

The family of central composite designs (CCD's) is the most commonly used experimental designs to fit second-order polynomials (Myers *et al*. 2009). The experimental design in CCD's consists of: (i) The 2^k factorial combinations in the 2^k factorial design at the levels ±1, (ii) 2k axial runs at levels ± α which is a one factor at a time array and (iii) the centre runs at the central levels of the factors denoted by '0'. Hence, the factors have five levels, viz. 0, ±1 and ± α. A particular case of the CCD is the FCD where α = 1. In this case, the factors have only three levels, which are 0 and ± 1. The combinations of the FCD lie at the corners as well as the centre of each of the faces of a k-dimensional hypercube which is centred on the combination of the centre points of all the factors (i.e., variables). The

Table 6 Design matrix for FCD

Run	Factor			Remarks
	X_1	X_2	X_3	
1	+1	+1	+1	The runs 1-8 correspond to the design matrix of the 2^k factorial design.
2	+1	+1	-1	
3	+1	-1	+1	
4	+1	-1	-1	
5	-1	+1	+1	
6	-1	+1	-1	
7	-1	-1	+1	
8	-1	-1	-1	
9	+1	0	0	The runs 9-14 correspond to the $2k$ axial runs with $\alpha = 1$.
10	-1	0	0	
11	0	+1	0	
12	0	-1	0	
13	0	0	+1	
14	0	0	-1	
15	0	0	0	The centre run

design matrix of the FCD with three factors X_1, X_2 and X_3 is also given in Table 6.

4.2.2 Multiple linear regression

The method of least squares is often used to estimate the β's and is adopted in the present study. The coefficient of multiple determination (R^2), adjusted R^2 (R^2_{adj}), R^2 for prediction (R^2_{pred}) and the mean square error (*MSE*) are some of the criteria for evaluating the regression model. In addition, the adequacy of the model is checked by ensuring that the residuals follow a normal distribution, thereby satisfying the normality assumption of linear regression. The Kolmogorov-Smirnov (K-S) test (Kolmogorov 1933, Smirnov 1939) is used for this purpose.

4.3 Monte carlo simulation (MCS) technique

In the present study, the MCS technique is also applied on the $g(X)$ approximated using the RSM to verify the accuracy of the H-L method. The MCS technique samples each of the random variables in the problem multiple times, according to the corresponding probabilistic characteristics. Each of these realisations of the random variables are then treated as separate realisations of the pile-slope system and the response of the system, $g(X)$, for each of these realisations is evaluated. If n number of such realisations are simulated, and 'n_f' events are observed with $g(X) < 0$, then the P_f can be computed as

$$P_f = \frac{n_f}{n} \tag{15}$$

provided n is sufficiently large.

5. Results and discussion

The results of sensitivity analysis (Fig. 10) show that the

Table 7 Summary of fit for multiple linear regression

X_p/X	S/D	Model	R^2	R^2_{adj}	R^2_{pred}	MSE
0.25	3.0	FOP	0.9811	0.9759	0.9567	0.0020
		SOP	0.9813	0.9672	0.9382	0.0027
	4.5	FOP	0.9680	0.9593	0.9224	0.0030
		SOP	0.9682	0.9443	0.9023	0.0040
	6.0	FOP	0.9697	0.9615	0.9300	0.0025
		SOP	0.9729	0.9526	0.9123	0.0031
0.50	3.0	FOP	0.9831	0.9785	0.9705	0.0031
		SOP	0.9903	0.9830	0.9628	0.0024
	4.5	FOP	0.9922	0.9900	0.9827	0.0011
		SOP	0.9937	0.9890	0.9790	0.0012
	6.0	FOP	0.9869	0.9833	0.9704	0.0017
		SOP	0.9883	0.9795	0.9620	0.0020
0.75	3.0	FOP	0.9647	0.9550	0.9338	0.0047
		SOP	0.9687	0.9453	0.8773	0.0058
	4.5	FOP	0.9836	0.9791	0.9683	0.0017
		SOP	0.9901	0.9827	0.9684	0.0014
	6.0	FOP	0.9739	0.9667	0.9386	0.0023
		SOP	0.9769	0.9596	0.9299	0.0028

FS is sensitive to the uncertainties in unit weight, cohesion and angle of internal friction of the soil. The performance function for the reliability analysis is approximated using polynomial basis expansion of these three random variables only. The performance function for the pile-slope system is expressed as

$$g(X) = FS_a - FS_t \tag{16}$$

where FS_a is the evaluated FS of the pile-slope system and X is the 3-dimensional vector [γ_s, c, ϕ].

5.1 Selection of the regression model

The relationship between the *FS* and the soil strength parameters can be considered to be linear (Zhang *et al.* 2017). The candidate polynomial models used to approximate the performance functions are given as

1. First-order polynomial (FOP) model:

$$g(X) = \beta_0 + \beta_1\gamma_s + \beta_2 c + \beta_3\phi - FS_t \tag{17}$$

2. Second-order polynomial (SOP) model:

$$g(X) = \beta_0 + \beta_1\gamma_s + \beta_2 c + \beta_3\phi + \beta_4\gamma_s^2 + \beta_5 c^2 + \beta_6\phi^2 - FS_t \tag{18}$$

In the above models, the last term FS_t is specified by the performance requirement and is constant. The rest of the terms correspond to FS_a. The pile-slope system shown in Fig. 6 is used to perform the reliability analysis. The FCD is used for the design of experiments. The factorial levels considered for the three variables in the reliability analysis are the same as in the case of sensitivity analysis. The

Table 8 K-S test and extra sum of squares test results

X_p/X	S/D	*KS*		F_0
		FOP	SOP	
0.25	3.0	0.169	0.177	0.025
	4.5	0.080	0.089	0.017
	6.0	0.131	0.153	0.323
0.50	3.0	0.154	0.114	2.000
	4.5	0.158	0.233	0.667
	6.0	0.115	0.218	0.333
0.75	3.0	0.117	0.097	0.345
	4.5	0.085	0.135	1.738
	6.0	0.068	0.132	0.345

corresponding values of FS_a are computed using ABAQUS for all the combinations mentioned in Table 6. The summary of fit for both the FOP and SOP models for all the combinations of pile locations and spacing is presented in Table 7. It is observed that the FOP model has superior statistics compared to the SOP model, except for the cases of X_p/X = 0.5 with S/D = 3.0 and X_p/X = 0.75 with S/D = 4.5, where the statistics are marginally better for the SOP model. However, even in these cases, the FOP model has very good R^2_{adj} values (0.9785 and 0.9791). Therefore it can be inferred that the FOP model is better than the SOP model because there is lesser unexplained variability in the first-order approximation compared to the second-order approximation.

In order to confirm the above, hypothesis test on the group of coefficients corresponding to the second order terms is performed using the 'extra sum of squares' method. The appropriate hypotheses for this test are

$$\begin{aligned} &H_0 : \beta_S = 0 \\ &H_1 : \beta_4 \neq 0 \text{ and/or } \beta_5 \neq 0 \text{ and/or } \beta_6 \neq 0 \end{aligned} \quad (19)$$

where $\beta_S = [\beta_4, \beta_5, \beta_6]$ are the partial regression coefficients corresponding to the second order terms in Eq. (18). The partial regression coefficients corresponding to the first order terms in Eq. (18) are denoted by β_F. The regression sum of squares (SS_R) due to β_S, given that β_F is already included in the model is given by

$$SS_R(\beta_S \mid \beta_F) = SS_R(\beta) - SS_R(\beta_F) \quad (20)$$

where β is the vector of partial regression coefficients of Eq. (18). If *MSE* is the mean square error of the SOP model and 'r' is the number of second order terms (in this case r = 3), then the null hypothesis H_0 can be tested by using the statistic:

$$F_0 = \frac{SS_R(\beta_S \mid \beta_F)/r}{MSE} \quad (21)$$

The H_0 is accepted if $F_0 < F_{\alpha,r,N-p}$ and the second order terms are deemed not contributing significantly to the model. Here, α is the significance level, 'N' is the sample size and 'p' is the number of regression coefficients in the SOP model. In the study, the hypothesis is tested for α = 0.05, N = 15 for the FCD with three variables, considering only one central run and p is 7 as in Eq. (18). The corresponding value of F, i.e., $F_{0.05,3,8}$ is equal to 4.066. The results of the hypothesis tests for all the combinations of pile locations and spacing are presented in Table 8. It is observed that the null hypothesis can be accepted for all the cases considered. Therefore it can be stated that the SOP model is not having superior predictive capability over the FOP model. Hence the response surface is approximated using the FOP model in the present study for reliability analysis.

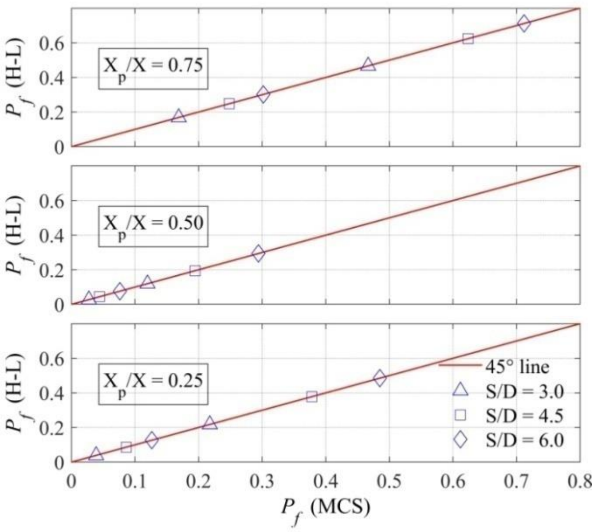

Fig. 12 Comparison of H-L method and MCS

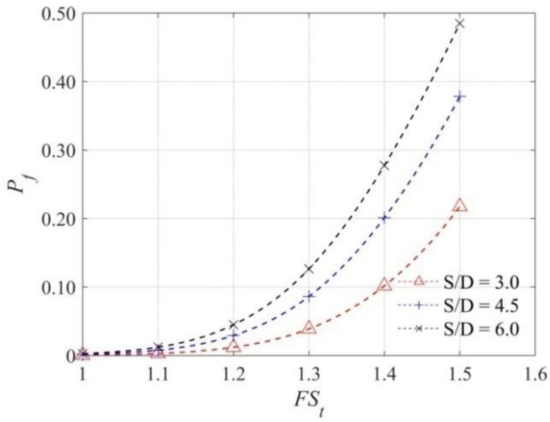

Fig. 13 P_f versus FS_t for X_p/X = 0.25

The K-S test statistic (*KS*) is reported in Table 8. The critical value of the test statistic (KS_α) for a significance level (α) of 0.05 is 0.340 for the sample size (N) of 15. It is observed that $KS < KS_\alpha$ for all the combinations of X_p/X and S/D ratios. The maximum value of *KS* observed for the first order approximations is 0.169, for X_p/X = 0.25 and S/D = 3.0. Therefore it can be inferred that the residuals satisfy the normality assumption.

5.2 Reliability analysis of the pile stabilised slope

The reliability index computed using the H-L method (β_{HL}) is used to find the P_f associated with the pile-slope

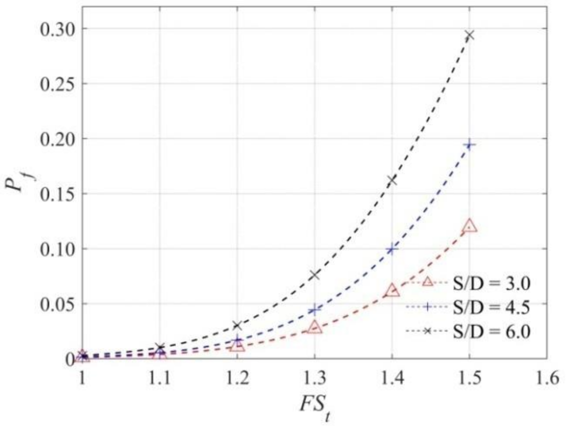

Fig. 14 P_f versus FS_t for $X_p/X = 0.50$

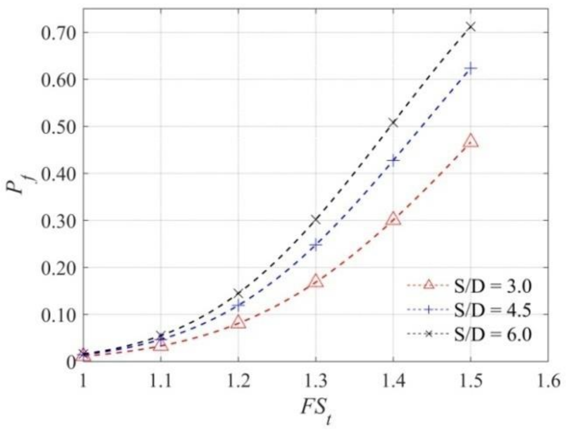

Fig. 15 P_f versus FS_t for $X_p/X = 0.75$

system as

$$P_f = \Phi(-\beta_{HL}) \tag{22}$$

where Φ represents the cumulative distribution function (CDF) of the standard normal variables. The MCS technique facilitates the evaluation of P_f in a direct way. The reliability analysis of the pile-slope system is carried out using both the methods. The results shown in Figs. 12-18 are computed using performance functions approximated with the data generated based on FCD. Comparison of the results of the H-L method and the MCS technique (n = 1 million) is shown in Fig. 12. For each of the combinations of X_p/X and S/D shown, the lower P_f corresponds to FS_t of 1.3 and the higher P_f corresponds to FS_t of 1.5. It is observed from the figure that the results of H-L method and MCS technique closely follow the 45° line and hence the results are in very good agreement.

The variation of P_f with FS_t for the different pile locations from the toe of the slope is shown in Figs. 13-15. It is observed that the P_f increases drastically with the increase in FS_t. This can be attributed to the fact that the P_f in this case is P($FS_a < FS_t$). Since the FS_a is approximated as a FOP function of the uncorrelated normal random variables γ_s, c and ϕ, the FS_a is also a normal random variable and accordingly the P_f values are evaluated. The P_f values follow the sigmoid shape of the Gauss error function (*erf*). Therefore a judicious selection of the FS_t is needed

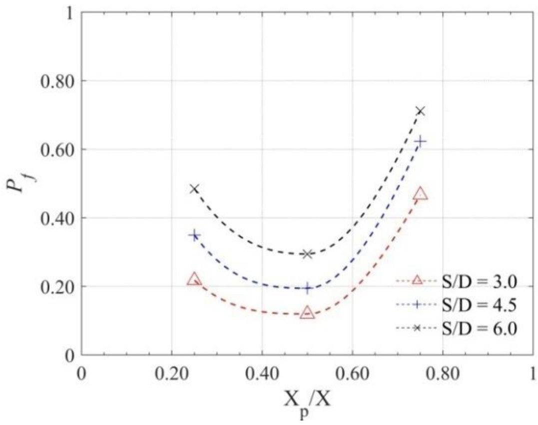

Fig. 16 Effect of location of row of piles on P_f

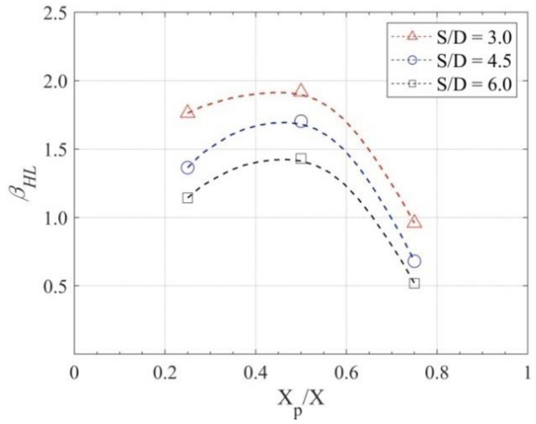

Fig. 17 Effect of location of row of piles on β_{HL}

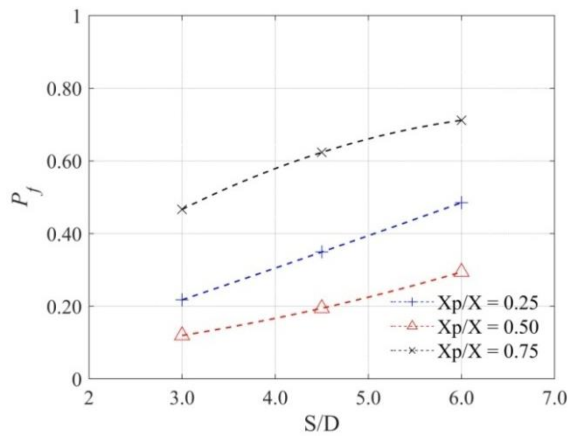

Fig. 18 Effect of pile spacing on P_f

while designing the pile-slope systems. It is to be noted that a slight increase in the FS_t may result in a drastic increase in the associated P_f of the pile-slope system.

The variation of P_f with the location of piles from the toe of the slope is shown in Fig. 16. The P_f values are shown for the FS_t of 1.5. The P_f is least for the case of row of piles located at the middle portion of the slope, irrespective of the spacing between the piles. This is consistent with the observation from Fig. 9 wherein the maximum FS is obtained for the case of piles placed at the middle portion of the slope. It is also noted that the general trend of the P_f matches with the observations of the

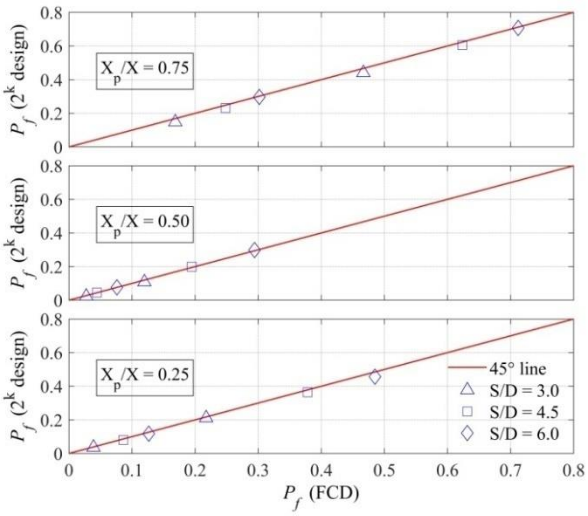

Fig. 19 Comparison of 2^k fact-centred design and FCD

deterministic analyses. The conformity between the deterministic and probabilistic results is better understood by drawing parallels between the *FS* and the analogous reliability index (β_{HL}). The variation of β_{HL} with the location of piles from the toe of the slope is shown in Fig. 17, which closely follows the trend of Fig. 9.

It is observed from Fig. 9 that all the pile configurations except for $X_p/X = 0.75$ with S/D ratios of 4.5 and 6.0, satisfy the performance criterion for FS_t of 1.5. The other pile configurations satisfy the performance criterion if the FS_t of 1.4 or lesser is chosen. However, it is seen from Fig. 16 that the P_f for the same FS_t differs for the different pile configurations. Hence it can be concluded that the reliability of the pile-slope system is not uniform and varies with the location of piles and spacing adopted, for the same FS_t. This indicates that the performance criterion should be specified as a combination of FS_t level and a stipulated minimum reliability index (or a maximum P_f).

The variation of the P_f with pile spacing is shown in Fig. 18 for the FS_t of 1.5. It can be seen that the P_f decreases with reduction in the pile spacing as the number of piles in the row per unit width of the slope increases. The increased number of piles offer more resistance to the sliding mass.

In the present study, it was decided to use the FCD, considering the possibility of curvature in the performance function, $g(X)$, over the 3D factorial space of the state variables, X. This would have necessitated the use of SOP to approximate the $g(X)$. However, it has been concluded that the $g(X)$ is sufficiently linear and hence modelled by FOP for the reliability analysis. The 2^k factorial design or 2^k factorial design augmented with a centre run (i.e., 2^k fact-centred design), with lesser number of runs with respect to the FCD would be sufficient to fit the FOP for approximating the $g(X)$. However a usual concern in this regard is the problem of possible lack of sufficient error degrees of freedom while performing the regression analysis. The error degrees of freedom must be sufficient enough for precise estimates of the partial regression coefficients β's. The error degrees of freedom for the 2^k fact-centred design, in the present study is 5 (N - k - 1), whereas for the FCD, it is 11. A trial is made in the study to understand the effect of lesser error degrees of freedom, if any, on the reliability analysis while using the 2^k fact-centred design. For this purpose, a comparison of the results of the P_f obtained from the reliability analyses using the data of 2^k fact-centred design and FCD matrices is shown in Fig. 19, where the 2^k fact-centred design is denoted by **2^k design**. For each of the combinations of X_p/X and S/D ratios selected, the lower P_f corresponds to FS_t of 1.3 and the higher P_f corresponds to FS_t of 1.5. It is observed that the results of the 2^k fact-centred design closely match with that of the FCD and the discrepancy between them is too small to warrant the use of FCD in the reliability analysis.

6. Conclusions

Reliability analysis of the stability of a soil slope reinforced with piles is performed in this study using the H-L method. Polynomial regression models are used to approximate the implicit performance function associated with the pile-slope system. The design matrices used for the multiple linear regression are based on the 2^k factorial design augmented with a centre run (2^k fact-centred design) and the FCD. The deterministic analyses are performed using 3D FEM for the generation of response data for the design matrix. The SRM is used along with FE analyses for the calculation of *FS*. The results of the reliability analyses are compared with the MCS technique involving 1 million simulations. The performance functions required in the MCS are approximated using the RSM. The following conclusions are made from the present study:

- The P_f obtained using the H-L method is in good agreement with the results of the MCS technique. It is concluded that the reliability analyses of the pile-slope systems can be performed efficiently using the H-L method.
- Both the 2^k fact-centred design and the FCD are equally good in approximating the FOP using multiple linear regression. The 2^k fact-centred design is sufficient for approximating the performance function using the FOP, provided the summary of fit data and the relevant hypothesis tests do not hint the possibility of curvature in the performance functions.
- The selected FS_t of the pile-slope system significantly affect the P_f associated with the system, especially at higher values of the FS_t. Therefore, the FS_t to be used in the design of pile-slope stabilisation system should be made based on the engineering judgement.
- The P_f of the pile-slope system is minimum when the piles are placed at the middle portion of the slope, irrespective of the spacing between the piles in the row. This is consistent with the results of the deterministic analyses for which the maximum *FS* are obtained. It is also noted that the P_f decreases with decrease in the spacing between the piles irrespective of the location of the row of piles from the toe of the slope.
- The different designs or pile configurations that satisfy the stability requirement of the pile-slope system with selected FS_t do not ensure the same P_f. Hence it is advocated to specify the performance criterion for the pile-slope system wherein one should select a minimum FS_t with an acceptable level of P_f.

References

ABAQUS/CAE (2014), *ABAQUS/CAE User's Guide*, Dassault Systèmes, Providence, Rhode Island, U.S.A.

Ausilio, E., Conte, E. and Dente, G. (2001), "Stability analysis of slopes reinforced with piles", *Comput. Geotech.*, **28**(8), 591-611. https://doi.org/10.1016/S0266-352X(01)00013-1.

Babu, G.L.S. and Singh, V.P. (2010), "Reliability analysis of a prototype soil nail wall using regression models", *Geomech. Eng.*, **2**(2), 71-88. https://doi.org/10.12989/gae.2010.2.2.071.

Cai, F. and Ugai, K. (2000), "Numerical analysis of the stability of a slope reinforced with piles", *Soils Found.*, **40**(1), 73-84. https://doi.org/10.3208/sandf.40.73.

Carrubba, P., Maugeri, M. and Motta, E. (1989), "Esperienze in vera grandezza sul comportamento di pali per la stabilizzaaione di un pendio", *Proceedings of the 17th Convegno Nazionale di Geotechnica*, Taromina, Italy, June.

Chan, C.L. and Low, B.K. (2012), "Practical second-order reliability analysis applied to foundation engineering", *Int. J. Numer. Anal. Meth. Geomech.*, **36**(11), 1387-1409. https://doi.org/10.1002/nag.1057.

Chen, L.T. and Poulos, H.G. (1997), "Piles subjected to lateral soil movements", *J. Geotech. Geoenviron. Eng.*, **123**(9), 802-811. https://doi.org/10.1061/(ASCE)1090-0241(1997)123:9(802).

Ellis, E.A., Durrani, I.K. and Reddish, D.J. (2010), "Numerical modelling of discrete pile rows for slope stability and generic guidance for design", *Geotechnique*, **60**(3), 185-195. https://doi.org/10.1680/geot.7.00090.

Eschenbach, T.G. (1992), "Spiderplots versus tornado diagrams for sensitivity analysis", *Interfaces*, **22**(6), 40-46. https://doi.org/10.1287/inte.22.6.40.

Griffiths, D.V. and Lane, P.A. (1999), "Slope stability analysis by finite elements", *Geotechnique*, **49**(3), 387-403. https://doi.org/10.1680/geot.1999.49.3.387.

GuhaRay, A. and Baidya, D.K. (2014), "Partial safety factors for retaining walls and slopes: A reliability based approach", *Geomech. Eng.*, **6**(2), 99-115. https://doi.org/10.12989/gae.2014.6.2.099.

Guo, W.D. and Ghee, E.H. (2004), "Response of free-head piles due to lateral soil movement", *Proceedings of the 9th Australia New Zealand Conference on Geomechanics*, Auckland, New Zealand, February.

Hamby, D.M. (1994), "A review of techniques for parameter sensitivity analysis of environmental models", *Environ. Monit. Assess.*, **32**(2), 135-154. https://doi.org/10.1007/BF00547132.

Hamrouni, A., Dias, D. and Sbartai, B. (2018), "Reliability analysis of a mechanically stabilized earth wall using the surface response methodology optimized by a genetic algorithm", *Geomech. Eng.*, **15**(4), 937-945. https://doi.org/10.12989/gae.2018.15.4.937.

Hasofer, A.M. and Lind, N.C. (1974), "Exact and invariant second-moment code format", *J. Eng. Mech. Div.*, **100**(1), 111-121.

Hassiotis, S., Chameau, J.L. and Gunaratne, M. (1997), "Design method for stabilization of slopes with piles", *J. Geotech. Geoenviron. Eng.*, **123**(4), 314-323. https://doi.org/10.1061/(ASCE)1090-0241(1997)123:4(314).

He, Y., Hazarika, H., Yasufuku, N., Teng, J., Jiang, Z. and Han, Z. (2015), "Estimation of lateral force acting on piles to stabilize landslides", *Nat. Hazards*, **79**(3), 1981-2003. https://doi.org/10.1007/s11069-015-1942-0.

Ho, I. (2014), "Parametric studies of slope stability analyses using three-dimensional finite element technique: Geometric effect", *J. GeoEng.*, **9**(1), 33-43. http://doi.org/10.6310/jog.2014.9(1).4.

Ho, I. (2015), "Numerical study of slope-stabilizing piles in undrained clayey slopes with a weak thin layer", *Int. J. Geomech.*, **15**(5), 234-249. https://doi.org/10.1061/(ASCE)GM.1943-5622.0000445.

Ho, I. (2017), "Three-dimensional finite element analysis for soil slopes stabilisation using piles", *Geomech. Geoeng.*, **12**(4), 234-249. https://doi.org/10.1080/17486025.2017.1347286.

Ito, T. and Matsui, T. (1975), "Methods to estimate lateral force acting on stabilizing piles", *Soils Found.*, **15**(4), 43-59. https://doi.org/10.3208/sandf1972.15.4_43.

Ito, T., Matsui, T. and Hong, W.P. (1981), "Design method for stabilizing piles against landslide - one row of piles", *Soils Found.*, **21**(1), 21-37. https://doi.org/10.3208/sandf1972.21.21.

Ji, J. and Low, B.K. (2012), "Stratified response surfaces for system probabilistic evaluation of slopes", *J. Geotech. Geoenviron. Eng.*, **138**(11), 1398-1406. https://doi.org/10.1061/(ASCE)GT.1943-5606.0000711.

Joorabchi, A.E. (2011), "Landslide stabilization using drilled shaft in static and dynamic condition", Ph.D. Dissertation, The University of Akron, Akron, Ohio, U.S.A.

Kolmogorov, A.N. (1933), "Sulla determinazione empirica di una legge di distribuzione", *Giornale dell'Istituto Italiano degli Attuari*, **4**, 83-91.

Lee, B.J., Kee, S., Oh, T. and Kim, Y. (2017), "Evaluating the dynamic elastic modulus of concrete using shear-wave velocity measurements", *Adv. Mater. Sci. Eng.* https://doi.org/10.1155/2017/1651753.

Lee, C.Y., Hull, T.S. and Poulos, H.G. (1995), "Simplified pile-slope stability analysis", *Comput. Geotech.*, **17**(1), 1-16. https://doi.org/10.1016/0266-352X(95)91300-S.

Li, D., Zheng, D., Cao, Z., Tang, X. and Phoon, K. (2016), "Response surface methods for slope reliability analysis: Review and comparison", *Eng. Geol.*, **203**, 3-14. https://doi.org/10.1016/j.enggeo.2015.09.003.

Li, L. and Liang, R.Y. (2014), "Reliability-based design for slopes reinforced with a row of drilled shafts", *Int. J. Numer. Anal. Meth. Geomech.*, **38**(2), 202-220. https://doi.org/10.1002/nag.2220.

Li, X., He, S., Luo, Y. and Wu, Y. (2011), "Numerical studies of the position of piles in slope stabilization", *Geomech. Geoeng.*, **6**(3), 209-215. https://doi.org/10.1080/17486025.2011.578668.

Li, X., Pei, X., Gutierrez, M. and He, S. (2012), "Optimal location of piles in slope stabilization by limit analysis", *Acta Geotechnica*, **7**(3), 253-259. https://doi.org/10.1007/s11440-012-0170-y.

Li, X., Su, L., He, S. and Xu, J. (2015), "Limit equilibrium analysis of seismic stability of slopes reinforced with a row of piles", *Int. J. Numer. Anal. Meth. Geomech.*, **40**(8), 1241-1250. https://doi.org/10.1002/nag.2484.

Loucks, D.P. and Van Beek, E. (2017), *Water Resource Systems Planning and Management: An Introduction to Methods, Models and Applications*, Springer, Cham, Zug, Switzerland.

Mandali, A.M., Sujith, M.S., Rao, B.N. and Maganti, J. (2011), "Reliability analysis of counterfort retaining walls", *Electron. J. Struct. Eng.*, **11**(1), 42-56.

Mangalathu, S., Jeon, J. and DesRoches, R. (2018), "Critical uncertainty parameters influencing seismic performance of bridges using lasso regression", *Earthq. Eng. Struct. Dyn.*, **47**(3), 784-801. https://doi.org/10.1002/eqe.2991.

McGann, C.R., Arduino, P. and Mackenzie-Helnwein, P. (2012), "Simplified procedure to account for a weaker soil layer in lateral load analysis of single piles", *J. Geotech. Geoenviron. Eng.*, **138**(9), 1129-1137. https://doi.org/10.1061/(ASCE)GT.1943-5606.0000684.

Myers, R.H., Montgomery, D.C. and Anderson-Cook, C.M. (2009), *Response Surface Methodology: Process and Product Optimization Using Designed Experiments*, John Wiley and Sons, Inc., Hoboken, New Jersey, U.S.A.

Ni, P., Mangalathu, S. and Liu, K. (2020), "Enhanced fragility

analysis of buried pipelines through lasso regression", *Acta Geotechnica*, **15**(2), 471-487. https://doi.org/10.1007/s11440-018-0719-5.
Ni, P., Mangalathu, S. and Yi, Y. (2018a), "Fragility analysis of continuous pipelines subjected to transverse permanent ground deformation", *Soils Found*., **58**(6), 1400-1413. https://doi.org/10.1016/j.sandf.2018.08.002.
Ni, P., Mangalathu, S., Mei, G. and Zhao, Y. (2017), "Permeable piles: An alternative to improve the performance of driven piles", *Comput. Geotech*., **84**, 78-87. https://doi.org/10.1016/j.compgeo.2016.11.021.
Ni, P., Mei, G. and Zhao, Y. (2018b), "Influence of raised groundwater level on the stability of unsaturated soil slopes", *Int. J. Geomech*., **18**(12), 04018168. https://doi.org/10.1061/(ASCE)GM.1943-5622.0001316.
Ni, P., Song, L., Mei, G. and Zhao, Y. (2018c), "On predicting displacement-dependent earth pressure for laterally loaded piles", *Soils Found*., **58**(1), 85-96. https://doi.org/10.1016/j.sandf.2017.11.007.
Ni, P., Wang, S., Zhang, S. and Mei, L. (2016), "Response of heterogeneous slopes to increased surcharge load", *Comput. Geotech*., **78**, 99-109. http://doi.org/10.1016/j.compgeo.2016.05.007.
Nian, T.K., Chen, G.Q., Luan. M.T., Yang, Q. and Zheng, D.F. (2008), "Limit analysis of the stability of slopes reinforced with piles against landslide in nonhomogenous and anisotropic soils", *Can. Geotech. J*., **45**(8), 1092-1103. https://doi.org/10.1139/T08-042.
Nowak, A.S. and Collins, K.R. (2013), *Reliability of Structures*, CRC Press, Boca Raton, Florida, U.S.A.
Phoon, K. and Kulhawy, F.H. (1999), "Characterization of geotechnical variability", *Can. Geotech. J*., **36**(4), 612-624. https://doi.org/10.1139/t99-038.
Poulos, H.G. (1995), "Design of reinforcing piles to increase slope stability", *Can. Geotech. J*., **32**(5), 808-818. https://doi.org/10.1139/t95-078.
Ruiz, S.E. (1984), "Reliability index for offshore piles subjected to bending", *Struct. Safety*, **2**(2), 83-90. https://doi.org/10.1016/0167-4730(84)90012-2.
Sayed, S., Dodagoudar, G.R. and Rajagopal, K. (2010), "Finite element reliability analysis of reinforced retaining walls", *Geomech. Geoeng*., **5**(3), 187-197. https://doi.org/10.1080/17486020903576788.
Shin, E.C., Patra, C.R. and Rout, A.K. (2006), "Automated stability analysis of slopes stabilized with piles", *KSCE J. Civ. Eng*., **10**(5), 333-338. https://doi.org/10.1007/BF02830087.
Smethurst, J.A. and Powrie, W. (2007), "Monitoring and analysis of the bending behaviour of discrete piles used to stabilise a railway embankment", *Geotechnique*, **57**(8), 663-677. https://doi.org/10.1680/geot.2007.57.8.663.
Smirnov, N.V. (1939), "Estimate of deviation between empirical distribution functions in two independent samples", *Bull. Moscow Univ*., **2**(2), 3-16.
Tu, Y., Liu, X., Zhong, Z. and Li, Y. (2016), "New criteria for defining slope failure using the strength reduction method", *Eng. Geol*., **212**, 63-71. https://doi.org/10.1016/j.enggeo.2016.08.002.
Wei, W.B. and Cheng, Y.M. (2009), "Strength reduction analysis for slope reinforced with one row of piles", *Comput. Geotech*., **36**(7), 1176-1185. https://doi.org/10.1016/j.compgeo.2009.05.004.
Won, J., You, K., Jeong, S. and Kim, S. (2005), "Coupled effects in stability analysis of pile-slope systems", *Comput. Geotech*., **32**(4), 304-315. https://doi.org/10.1016/j.compgeo.2005.02.006.
Xu, J., Li, Y. and Yang, X. (2018), "Stability charts and reinforcement with piles in 3D nonhomogeneous and anisotropic soil slope", *Geomech. Eng*., **14**(1), 71-81. https://doi.org/10.12989/gae.2018.14.1.071.
Yang, X.L. and Li, W.T. (2017), "Reliability analysis of shallow tunnel with surface settlement", *Geomech. Eng*., **12**(2), 313-326. https://doi.org/10.12989/gae.2017.12.2.313.
Yang, X.L. and Liu, Z.A. (2018), "Reliability analysis of three-dimensional rock slope", *Geomech. Eng*., **15**(6), 1183-1191. https://doi.org/10.12989/gae.2018.15.6.1183.
Yu, Y., Shang, Y. and Sun, H. (2014), "A theoretical method to predict crack initiation in stabilizing piles", *KSCE J. Civ. Eng*., **18**(5), 1332-1341. https://doi.org/10.1007/s12205-014-0063-8.
Zhang, B., Ma, Z., Wang, X., Zhang, J. and Peng, W. (2020), "Reliability analysis of anti-seismic stability of 3D pressurized tunnel faces by response surfaces method", *Geomech. Eng*., **20**(1), 43-54. https://doi.org/10.12989/gae.2020.20.1.043.
Zhang, J., Huang, H.W., Juang, C.H. and Li, D.Q. (2013), "Extension of Hassan and Wolff method for system reliability analysis of soil slopes", *Eng. Geol*., **160**, 81-88. https://doi.org/10.1016/j.enggeo.2013.03.029.
Zhang, J., Wang, H., Huang, H.W. and Chen, L.H. (2017), "System reliability analysis of soil slopes stabilized with piles", *Eng. Geol*., **229**, 45-52. https://doi.org/10.1016/j.enggeo.2017.09.009.
Zhou, C., Shao, W. and van Westen, C.J. (2014), "Comparing two methods to estimate lateral force acting on stabilizing piles for a landslide in the Three Gorges reservoir, China", *Eng. Geol*., **173**, 41-53. https://doi.org/10.1016/j.enggeo.2014.02.004.
Zhu, J.Q. and Yang, X.L. (2018), "Probabilistic stability analysis of rock slopes with cracks", *Geomech. Eng*., **16**(6), 655-667. https://doi.org/10.12989/gae.2018.16.6.655.
Zienkiewicz, O.C., Humpheson, C. and Lewis, R.W. (1975), "Associated and non-associated visco-plasticity and plasticity in soil mechanics", *Geotechnique*, **25**(4), 671-689. https://doi.org/10.1680/geot.1975.25.4.671.

CC